ORIGINAL ARTICLE

Hyperglycemia Enhances IGF-I–Stimulated Src Activation via Increasing Nox4-Derived Reactive Oxygen Species in a PKCζ-Dependent Manner in Vascular Smooth Muscle Cells

Gang Xi, Xinchun Shen, Laura A. Maile, Christine Wai, Katherine Gollahon, and David R. Clemmons

IGF-I–stimulated sarcoma viral oncogene (Src) activation during hyperglycemia is required for propagating downstream signaling. The aim of the current study was to determine the mechanism by which hyperglycemia enhances IGF-I–stimulated Src activation and the role of NADPH oxidase 4 (Nox4) and protein kinase C ζ (PKCζ) in mediating this response in vascular smooth muscle cells (VSMCs). Nox4 expression was analyzed in VSMCs exposed to hyperglycemia. The role of Nox4-derived reactive oxygen species (ROS) in IGF-I–stimulated Src activation was investigated via knockdown of Nox4. Different isoforms of PKC were screened to investigate their role in hyperglycemia-induced Nox4. The oxidation of Src was shown to be a prerequisite for its activation in response to IGF-I during hyperglycemia. Hyperglycemia induced Nox4, but not Nox1, and p22 phagocyte oxidase (p22phox) expression and IGF-I stimulated Nox4/p22phox complex formation, leading to increased ROS generation. Knockdown of Nox4 prevented ROS generation and impaired the oxidation and activation of Src in response to IGF-I, whereas knockdown of Nox1 had no effect. PKCζ was shown to mediate the hyperglycemia-induced increase in Nox4 expression. The key observations in cultured VSMCs were confirmed in the diabetic mice. Nox4-derived ROS is responsible for the enhancing effect of hyperglycemia on IGF-I–stimulated Src activation, which in turn amplifies IGF-I–linked downstream signaling and biological actions. ***Diabetes*** **61:104–113, 2012**

Hyperglycemia is a risk factor for diabetes complications (1). Inhibition of hyperglycemia-induced reactive oxygen species (ROS) generation attenuates these changes (2). In vascular smooth muscle cells (VSMCs), hyperglycemia enhances the cellular responsiveness to IGF-I, including increased cell proliferation and migration (3), processes that contribute to atherosclerosis (4). VSMCs adapt to hyperglycemia by changing the signaling components that respond to IGF-I stimulation (5). The induction of sarcoma viral oncogene (Src) kinase is one of these changes (6,7), and activated Src has been linked to diabetic vascular complications (8).

The Src kinase domain is maintained in an inactive state by intramolecular interactions (9,10) and activated by disruption of these interactions with high-affinity ligands (11,12). Changing Src oxidation has been proposed as an important factor for regulating Src activation (13,14). Src undergoes activation after oxidation of Cys245 and Cys487 during focal adhesion formation (15), and exposure of platelets to hydrogen peroxide induces Src activation (16). ROS are generated in a variety of conditions that are associated with increased cell proliferation/migration (17). In vascular cells, NADPH oxidase (Nox) is a major source for intracellular ROS generation (18). Nox4 is one of the major isoforms in vascular cells (19), and Nox4-derived ROS has been shown to be required for Src activation in response to angiotensin-II (14). However, the mechanism by which the Nox4-mediated increase in ROS leads to Src activation was not determined.

In VSMCs, Nox4 has been shown to be associated with an IGF-I–stimulated increase in ROS generation (20). Additionally, high glucose has been shown to increase Nox4 expression in mesangial (21) and endothelial cells (22) in a protein kinase C (PKC)–dependent manner. Therefore, we investigated the relative roles of high glucose and IGF-I in the induction of Nox4 activation and ROS generation, and determined which PKC isoform mediates these changes. Furthermore, we determined the mechanism by which hyperglycemia enhances IGF-I–stimulated Src oxidation and kinase activation and verified the importance of these changes in blood vessels of diabetic mice.

RESEARCH DESIGN AND METHODS

Human IGF-I was a gift from Genentech (South San Francisco, CA). The anti-Src and 2, 4-dinitrophenyl antibodies were purchased from Millipore Corp. (Billerica, MA). Dulbecco's modified Eagle's medium (DMEM) containing 25 mmol/L glucose, and 5 mmol/L glucose, streptomycin, penicillin, 2′, 7′-dichlorofluorescein diacetate, and the Amplex red hydrogen peroxide assay kit were purchased from Invitrogen (Carlsbad, CA). PD98059, protein kinase B (AKT) inhibitor, BAY 11-7082, Gö 6976, PKCε inhibitor, and the PKCζ pseudosubstrate inhibitor were obtained from EMD Bioscience (San Diego, CA). The anti-Src homology collagen (Shc) antibody was purchased from BD Bioscience (San Diego, CA). Antibodies against phospho-AKT (Ser 473), total AKT, pSrc (Tyr 419), pErk1/2 (Thr202/Tyr204), and Erk1/2 (extracellular signal–related kinase 1/2) were from Cell Signaling Technology, Inc. (Beverly, MA). Anti–p22 phagocyte oxidase (p22phox), PY99, β-actin, PKCζ, and IGF-I receptor antibodies were purchased from Santa Cruz Biotechnology, Inc. (Santa Cruz, CA). Anti-Nox1, Nox4, and Ki67 antibodies were purchased from Abcam (Cambridge, MA). All other reagents were obtained from Sigma-Aldrich (St. Louis, MO) unless otherwise stated.

Construction of cDNAs and establishment of Nox4 silenced (Si), PKCζ Si, Nox1 Si, and β-D-galactosidase (LacZ) Si cells. Based on the Invitrogen website design tools, the oligonucleotides GGTGTATCCGGAGCAATAAAC, GCCAGTGCAGCGAAAGGATAT, GGACAACCTGGCACTATTTG, and GCTACACAAATCAGCGATTT were used to construct the short hairpin RNA (shRNA) template plasmids to knock down Nox4, PKCζ, Nox1, and LacZ, respectively. Plasmid construction, viral stock preparation, and transfection of VSMCs expressing the corresponding shRNAs followed procedures described previously (23).

Immunoprecipitation and immunoblotting. The cell monolayers were lysed in a modified radioimmunoprecipitation assay buffer (24). Immunoprecipitation was performed by incubating 0.5 mg cell lysate protein (determined by

From the Department of Medicine, University of North Carolina School of Medicine, Chapel Hill, North Carolina.
Corresponding author: David R. Clemmons, david_clemmons@med.unc.edu.
Received 18 July 2011 and accepted 23 October 2011.
DOI: 10.2337/db11-0990
This article contains Supplementary Data online at http://diabetes.diabetesjournals.org/lookup/suppl/doi:10.2337/db11-0990/-/DC1.

bicinchoninic acid assay (BCA) according to the manufacturer's instructions; Thermo Fisher Scientific , [Rockford, IL]) with 1 μg of corresponding antibody at 4°C overnight. Immunoblotting was performed as described previously (24).

Measurement of intracellular ROS level. Intracellular ROS was measured using the DFC-DA assay as described previously (24). For *N*-acetyl-cysteine (NAC) treatment, 2 mmol/L NAC was added 18–20 h before IGF-I exposure or ROS measurement. Diphenyleneiodonium (DPI; 10 nmol/L) was added 1 h before IGF-I exposure or ROS measurement. Intracellular hydrogen peroxide was measured using an Amplex red assay according to the manufacturer's instructions.

Measurement of protein oxidation level. Protein oxidation was measured using a modified OxyBlot protein detection kit (Millipore). After the immunoprecipitation of Src, the protein was released from the protein A beads using 12% SDS. Protein (10 μg) was derivatized with 20 μl 1× dinitrophenylhydrazine at room temperature for 15 min. The reaction was stopped by adding 15 μl neutralization solution and separated by a 7.5% polyacrylamide gel.

In vitro Src kinase assay. Src kinase activity was determined in vitro using a Src kinase assay kit (Millipore) according to a procedure described previously (23).

Animal preparations and treatments. Animal maintenance conformed to the U.S. National Institutes of Health Guide for the Care and Use of Laboratory Animals. Hyperglycemia was induced in C57/B6 mice (Taconic, Hudson, NY) using streptozotocin as described previously (25). Mice that had serum glucose concentrations >250 mg/dL were considered diabetic. After induction of diabetes, they were maintained for 2 weeks before any treatment. Based on a published report (26), the animals received the PKCζ inhibitor (n = 12) (2 mg/kg i.p.) administered daily for 2 days before being killed. IGF-I (1 mg/kg i.p. (n = 18) was administered 24 h for Ki67 staining and 15 min before being killed for assessment of the signal transduction. The mice were fasted overnight (16 h) before being killed.

Preparation of aortas for analysis. The mice were killed by injection of Nembutal (100 mg/kg i.p.) before harvesting the aortas. The thoracic aortas were harvested and placed into ice-cold PBS. Connective tissue and endothelium were removed before protein extraction or fixation. For biochemical analyses, the aortas were homogenized in ice-cold buffer (20 mmol/L Tris, 150 mmol/L sodium chloride, 2 mmol/L EDTA, and 0.05% Triton X-100, pH 7.4) using a glass tissue grinder.

Immunohistochemistry. The aortas from mice were fixed with 4% paraformaldehyde overnight, and paraffin embedded sections were prepared by the University of North Carolina Histology Core Facility. Antigen retrieval from the paraffin-embedded sections was performed using Tris/EDTA buffer (pH 9.0) and a programmed decloaking chamber (Biocare Medical, Concord, CA) before incubation with an anti-Ki67 antibody (3 μg/mL). This was followed by incubating with a biotin-conjugated goat anti-rabbit secondary antibody (1:2,000) and horseradish peroxidase–conjugated avidin (1:4,000), respectively. Staining was visualized using a DAB detection kit (Abcam). The Ki67-positive area in a whole aortic ring was quantified using NIH ImageJ and expressed as the percentage of the total area.

Cell proliferation assay. Assessment of VSMC proliferation was performed as described previously (27). For NAC treatment, NAC (2 mmol/L) was added for 18–20 h before IGF-I was added, and this was repeated after 24 h.

Cell migration assay. Cell migration assays were performed as described previously (28).

Statistical analysis. The Student t test was used to compare differences between control and one treatment or control cells and one mutant for most in vitro experiments. One or two-way ANOVA was applied for all data obtained from in vivo studies or when multiple treatments or multiple cell types were compared using data from in vitro studies. $P \leq 0.05$ was considered statistically significant.

RESULTS

Oxidation of Src is required for IGF-I–stimulated Src kinase activation. Hyperglycemia increased Src oxidation in VSMCs (192 ± 54% increase; $P < 0.01$) (Fig. 1*A*). IGF-I induced a further 64 ± 18% increase ($P < 0.01$). IGF-I had a minimal effect in VSMCs maintained in 5 mmol/L glucose. The antioxidant NAC prevented the IGF-I–induced increase in Src oxidation (Fig. 1*B*). IGF-I stimulated an 89 ± 19% increase ($P < 0.01$) in Src Y419 phosphorylation in high glucose but there was no significant change in cells maintained in normal glucose (Fig. 1*C*). Hyperglycemia alone did not increase Src activation significantly. Preincubation with NAC prevented the response to IGF-I plus hyperglycemia (Fig. 1*D*), but it had no effect on IGF-I receptor activation (Supplementary Fig. 1*A*). High glucose alone did not increase Src kinase activity (Fig. 1*E*) but H_2O_2 addition to cells cultured in normal glucose increased Src kinase (e.g., 22 ± 4% increase; $P < 0.05$). IGF-I significantly increased Src kinase activity in cells exposed to hyperglycemia (e.g., 186 ± 12 vs. 45 ± 8% in normal glucose; $P < 0.01$) and this was inhibited by NAC (e.g., 60 ± 3%; $P < 0.01$) (Fig. 1*E*). Similarly, when IGF-I was added with H_2O_2 to cells maintained in normal glucose, it stimulated a 120 ± 6% increase ($P < 0.001$) (Fig. 1*E*).

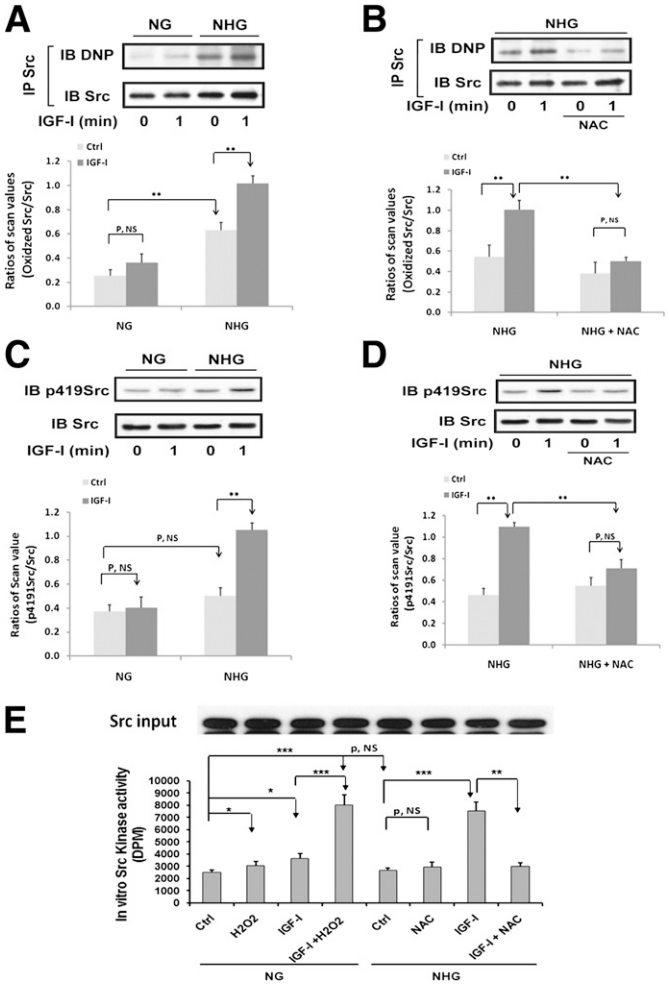

FIG. 1. Oxidation of Src is required for Src activation in response to IGF-I. VSMCs were isolated from porcine aortas using a method that has been described previously (50), cultured in DMEM containing normal glucose (NG; 5 mmol/L) plus 10% FBS (Hyclone, Logan, UT), and serum deprived for 16 h before treatment with 25 mmol/L glucose (NHG) for 24 h or maintained in NG in the presence or absence of IGF-I (100 ng/mL) for 1 min (*A–E*). For NAC treatment, 2 mmol/L NAC was preincubated for 1 h before adding glucose (*B*, *D*, and *E*). For H_2O_2 treatment, 200 μmol/L H_2O_2 was preincubated for 1 h before IGF-I exposure (*E*). *A* and *B*: Src was immunoprecipitated with an anti-Src antibody. Oxidized Src levels were measured according to the procedure described in RESEARCH DESIGN AND METHODS. To control for loading, the blots were stripped and probed with an anti-Src antibody (1:1,000 dilution). The proteins were visualized using enhanced chemiluminescence (Thermo Fisher Scientific). *C* and *D*: Cell lysates were immunoblotted with an anti-p419Src antibody (1:1,000). To control for loading, the blots were stripped and probed with an anti-Src antibody. *E*: Src protein was immunoprecipitated with an anti-Src antibody, and the immune complexes were used to measure in vitro Src kinase activity according to the procedure described in RESEARCH DESIGN AND METHODS. To control for Src protein input, after immunoprecipitation, the same amount of immune complexes from all treatments was immunoblotted with an anti-Src antibody. *$P < 0.05$, **$P < 0.01$, and ***$P < 0.001$ indicate significant differences between two treatments. The figures are representative of three independent experiments except *C* and *D*, which are representative of four.

ROS is required for Src oxidation and activation in response to IGF-I during hyperglycemia. ROS generation was significantly increased in 15 mmol/L glucose, and 25 mmol/L glucose induced greater increases (e.g., 279 ± 20% increase, $P < 0.01$, compared with 5 mmol/L glucose) (Fig. 2*A*). Mannitol had no effect. IGF-I stimulated an additional 73 ± 5% increase in ROS in cells exposed to 25 mmol/L glucose ($P < 0.01$), whereas its effect was minimal in normal glucose (Fig. 2*B*). NAC prevented this increase (Fig. 2*C*). Similar results were obtained using Amplex red (Supplementary Fig. 1*B* and *C*). When H_2O_2 was added to cells maintained in normal glucose, IGF-I–stimulated Src activation reached a level that was similar to the cells maintained in high glucose (Fig. 2*D*). The response to IGF-I plus H_2O_2 was prevented by NAC. H_2O_2 treatment also increased basal Src activation (e.g., 39 ± 13% increase; $P < 0.05$) (Fig. 2*D*).

High glucose induces Nox4 and p22phox expression, and IGF-I stimulates Nox4/p22phox complex formation. To examine whether the increase in ROS in response to IGF-I was due to Nox activation, DPI, a general Nox inhibitor, was used. DPI significantly inhibited ROS generation in response to high glucose (Supplementary Fig. 2*A* and *B*). DPI also prevented Src activation in response to IGF-I during hyperglycemia (Supplementary Fig. 2*C* and *D*).

Prior studies have shown that Nox1 and Nox4 are the predominant forms of Nox expressed in VSMCs (29,30). When VSMCs maintained in 5 mmol/L glucose were exposed to 25 mmol/L glucose, Nox4 expression increased after 6 h and reached a peak at 24 h (250 ± 30% increase; $P < 0.05$) (Supplementary Fig. 3*A*), whereas Nox1 increased only 70 ± 9% (Supplementary Fig. 3*B*). Increasing concentrations of glucose induced progressive increases in Nox4 expression (Fig. 3*A*). A similar pattern was observed in the expression of p22phox, which forms a complex with Nox4 to generate ROS. Because a short (e.g., 10 min) exposure to IGF-I had no effect on Nox4 expression (data not shown) but it enhanced ROS generation, we determined whether IGF-I could stimulate Nox4/p22phox complex formation. Nox4/p22phox complex formation was increased after 1 min of IGF-I stimulation in high glucose (Fig. 3*B*). To determine if hyperglycemia was required, we cultured the cells in normal glucose and then switched to high glucose for 24 h before IGF-I stimulation. This treatment enabled IGF-I to enhance Nox4/p22phox complex formation (e.g., a 184 ± 34% increase after 1 min; $P < 0.001$), whereas it had no effect at 1 min and it stimulated

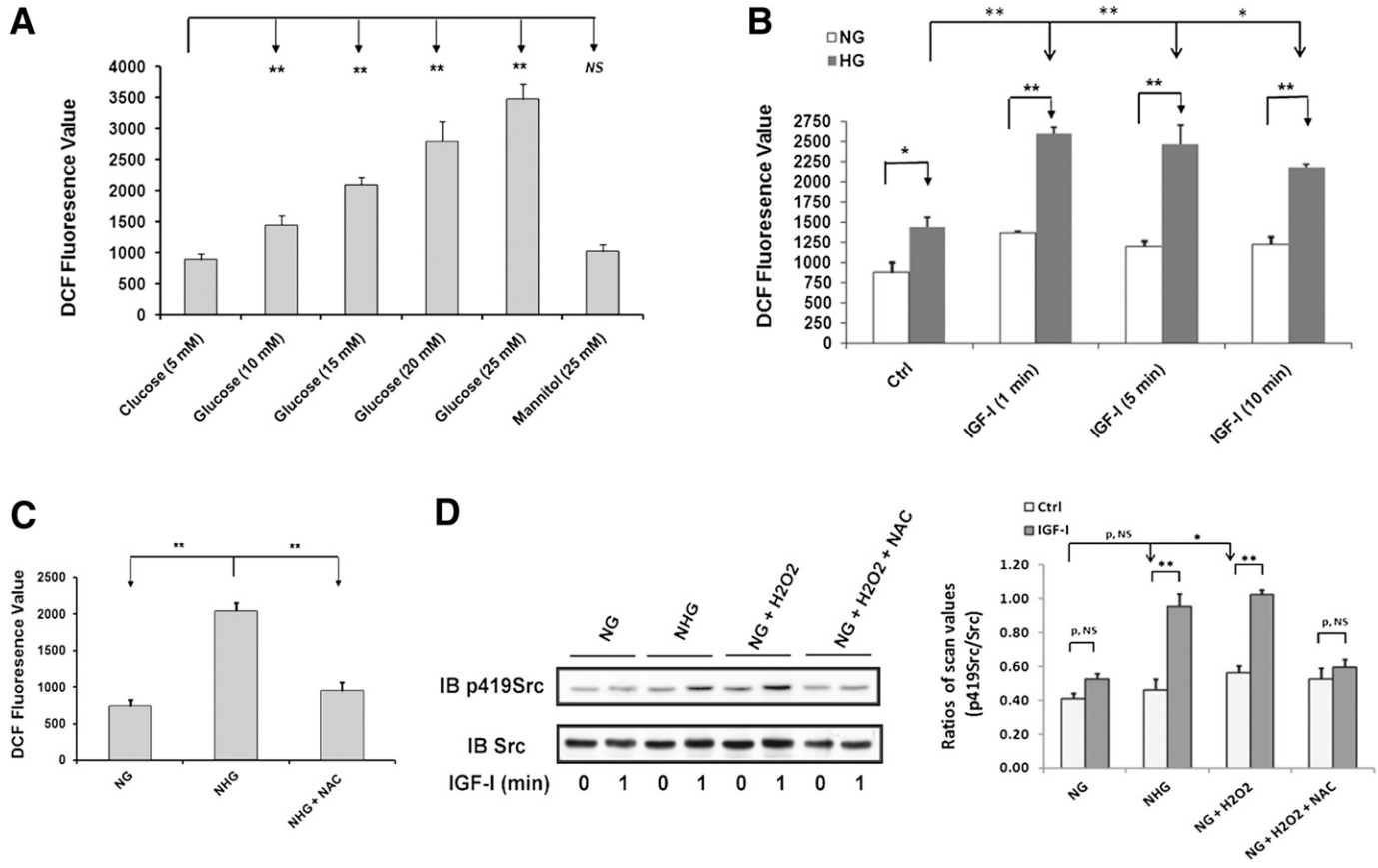

FIG. 2. Hyperglycemia- and IGF-I–induced ROS are required for Src activation in response to IGF-I during hyperglycemia. *A*: VSMCs were cultured in DMEM containing normal glucose (NG; 5 mmol/L) and serum starved for 16 h before addition of the indicated glucose concentration. Mannitol (25 mmol/L) was used as an osmotic control. *B*: VSMCs were cultured in DMEM containing high glucose (HG; 25 mmol/L) or NG (5 mmol/L) and serum starved for 16 h before addition of IGF-I (100 ng/mL) for the indicated times. *C*: Cells were cultured in DMEM containing NG plus 10% FBS and serum deprived for 16 h with DMEM containing NG or HG (NHG) before ROS measurement. NAC was added with serum-free DMEM and incubated for 16 h. ROS generation was determined according to the procedure described in RESEARCH DESIGN AND METHODS. *D*: Cells were cultured in DMEM containing NG plus 10% FBS and serum deprived for 16 h in DMEM containing NG or HG (NHG). For NAC treatment, 2 mmol/L NAC was added and incubated for 16 h before IGF-I treatment. H_2O_2 (200 μmol/L) was added for 1 h before IGF-I exposure for the indicated times. Cell lysates were immunoblotted with an anti-p419Src antibody and reprobed with an anti-Src antibody as a loading control. *$P < 0.05$ and **$P < 0.01$ indicate significant differences between two treatments. The figures are representative of three independent experiments.

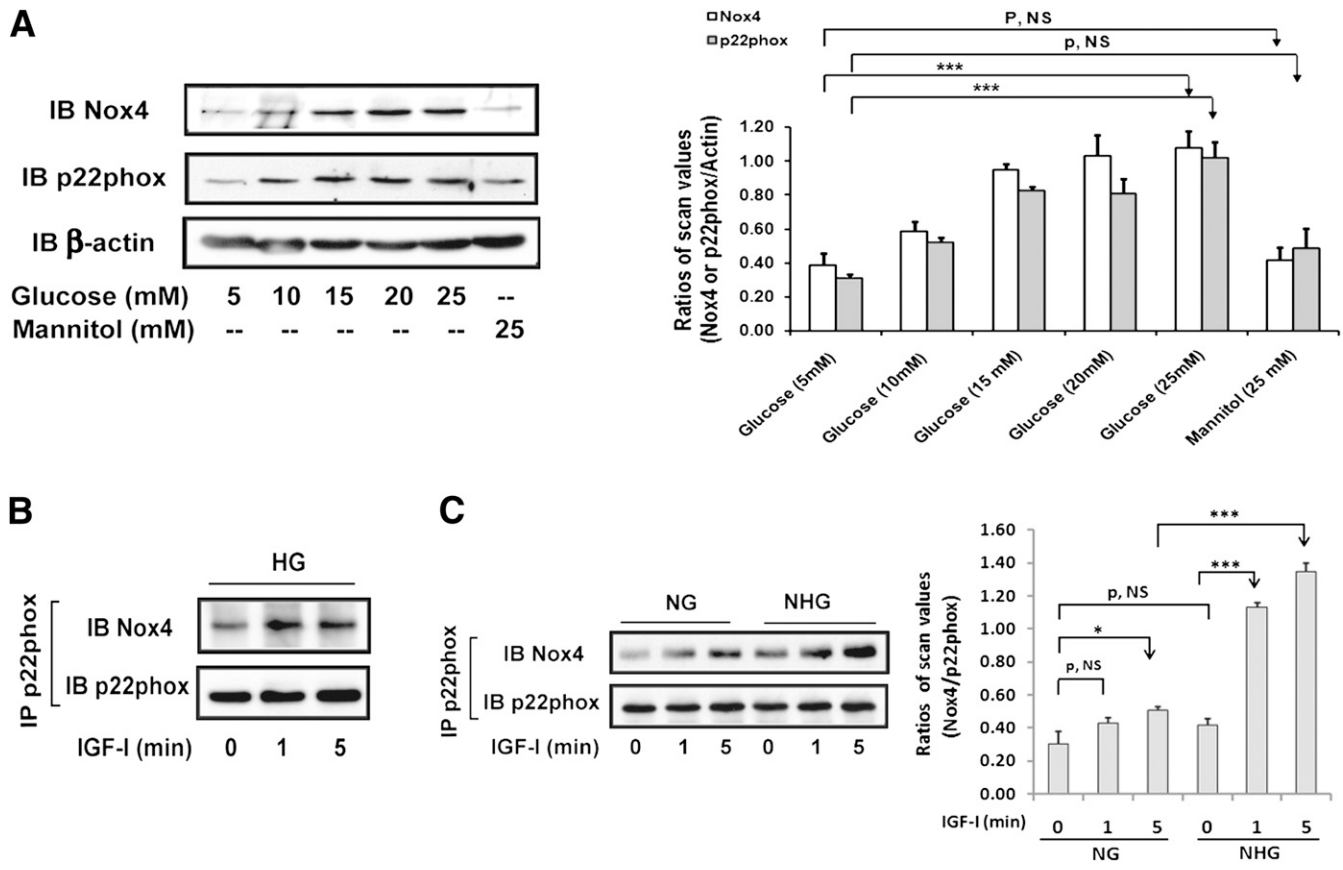

FIG. 3. Hyperglycemia induces Nox4 and p22phox expression, and IGF-I stimulates Nox4/p22phox complex formation during hyperglycemia. *A*: VSMCs were cultured in DMEM containing normal glucose (NG; 5 mmol/L) plus 10% FBS and serum deprived for 16 h before adding the indicated concentration of glucose. Mannitol (25 mmol/L) was used as an osmotic control. Cell lysates were immunoblotted with anti-Nox4 (1:500) and p22phox (1:1,000) antibodies. To control for loading, the blot was stripped and reprobed with an anti–β-actin (1:1,000) antibody. The value of each bar is the ratio of the scan value of Nox4 or p22phox divided by the value of β-actin, respectively. *B* and *C*: Cells were cultured in DMEM containing high glucose (HG; 25 mmol/L) or NG plus 10% FBS and serum deprived for 16 h before IGF-I treatment for the indicated times (*B*), or they were changed to 25 mmol/L glucose (NHG) or maintained in NG for 24 h in the presence or absence of IGF-I for the indicated times (*C*). Cell lysates were immunoprecipitated with an anti-p22phox antibody and immunoblotted with an anti-Nox4 antibody. To control loading, the blots were stripped and probed with an anti-p22phox antibody. The value of each bar is the ratio of the scan value of Nox4 divided by the value of p22phox. *P < 0.05 and ***P < 0.001 indicate significant differences between two treatments. The figures are representative of three independent experiments except *C*, which is representative of four.

only a 53 ± 25% increase after 5 min ($P < 0.05$) when cells were maintained in normal glucose (Fig. 3*C*). The absolute level of Nox4/p22phox complex formation was reduced by 62 ± 1% in cells maintained in normal glucose ($P < 0.001$). High glucose alone resulted in a nonsignificant change in Nox4/p22phox association. Inhibition of either mitogen-activated protein (MAP) kinase or AKT activation had no effect on IGF-I–stimulated Nox4/p22phox association (Supplementary Fig. 3*C*).

Nox4-derived ROS is required for Src oxidation and activation in response to IGF-I during hyperglycemia. To definitely determine that Nox4 is the isoform that is required for Src oxidation and activation, we used Nox4 shRNA. Nox4 expression was reduced ~90% (Fig. 4*A*), and silencing Nox4 did not alter the expression of p22phox or Nox1 (Fig. 4*A*). Knockdown of Nox4 did not affect IGF-I–stimulated IGF-I receptor phosphorylation (Supplementary Fig. 3*D*). Increasing the glucose concentration from 5 to 25 mmol/L stimulated Nox4 expression in LacZ knockdown cells by 155 ± 17% but it had no effect in cells expressing Nox4 shRNA (Fig. 4*B*). High glucose–induced ROS generation was reduced by 73 ± 6% ($P < 0.01$) in Nox4 knockdown cells compared with control cells, whereas the basal ROS level was not significantly different. This suggests that a Nox4-independent ROS generation pathway exists (Fig. 4*C*). Nox4 knockdown prevented IGF-I stimulation in Src oxidation (e.g., 22 ± 9% increase; P = NS) and activation (e.g., 29 ± 9% increase; P = NS), whereas in control cells, IGF-I induced significant changes (e.g., 111 ± 14%, $P < 0.05$, and 146 ± 12%, $P < 0.01$, increases, respectively) (Fig. 4*D* and *E*). IGF-I–stimulated Src kinase activity was reduced by 82 ± 4% ($P < 0.01$) compared with control cells exposed to high glucose, whereas knockdown Nox4 had no effect on IGF-I–stimulated Src activation when cells were exposed to normal glucose (Fig. 4*F*).

High glucose induces Nox4 expression in a PKCζ-dependent manner. To determine the PKC isoform that mediates the high glucose–induced increase in Nox4 expression, several PKC inhibitors were used. Only the PKCζ inhibitor prevented the high glucose–induced increase of Nox4 (Fig. 5*A*) and IGF-I–stimulated Src activation (Fig. 5*B*). To definitively determine if PKCζ mediates high glucose–induced Nox4 expression, we knocked down PKCζ and obtained a 90% reduction (Fig. 5*C*). Knockdown of PKCζ prevented high glucose–induced Nox4 expression (Fig. 5*D*), ROS generation (Supplementary Fig. 4*A*), and IGF-I–stimulated Src oxidation (Fig. 5*E*) and activation

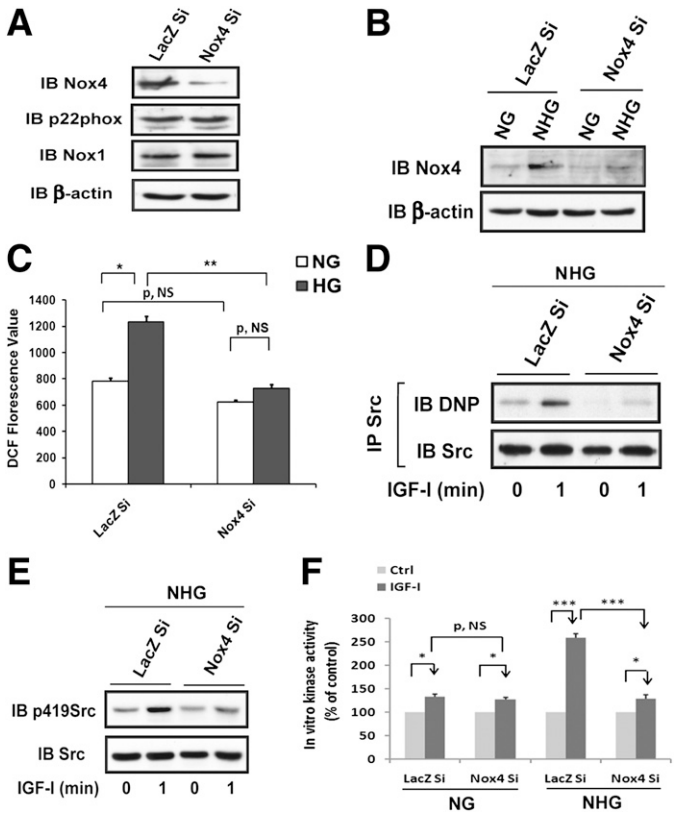

FIG. 4. Knockdown Nox4 prevents hyperglycemia-induced Nox4-derived ROS generation and IGF-I–stimulated Src oxidation and activation. VSMCs expressing shRNA targeting LacZ (LacZ Si) and Nox4 (Nox4 Si) were cultured in DMEM containing high glucose (HG; 25 mmol/L). *A*: Cell lysates were immunoblotted with anti-Nox4, p22phox, Nox1(1:500), and β-actin antibodies. *B*, *D*, *E* and *F*: Cells were cultured in the DMEM containing normal glucose (NG; 5 mmol/L), serum deprived for 16 h, and then changed from NG to HG (NHG; 25 mmol/L) or maintained in NG and incubated for 24 h before IGF-I exposure. *B*: Cell lysates were immunoblotted with anti-Nox4 and β-actin antibodies. *C*: Cells were cultured in DMEM containing NG or HG and serum deprived for 16 before measuring ROS levels. ROS measurement was determined according to the procedure described in RESEARCH DESIGN AND METHODS. *D*: Src was immunoprecipitated with an anti-Src antibody, and protein oxidation level was measured according to the procedure described in RESEARCH DESIGN AND METHODS. To control for loading, the blot was stripped and reprobed with an anti-Src antibody. *E*: Cell lysates were immunoblotted with an anti-p419Src antibody and reprobed with an anti-Src antibody as a loading control. *F*: Cell lysates were immunoprecipitated with an anti-Src antibody before measuring the in vitro kinase activity according to the procedure described in RESEARCH DESIGN AND METHODS. *$P < 0.05$, **$P < 0.01$, and ***$P < 0.001$ indicate significant differences between two cell types or treatments. The figures are representative of three independent experiments.

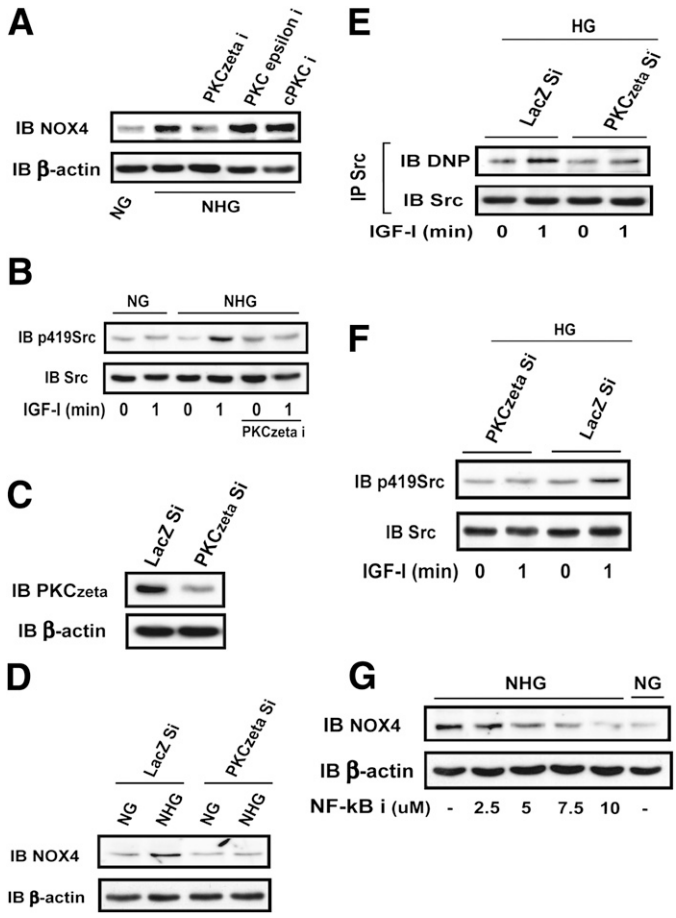

FIG. 5. PKCζ mediates high glucose (HG)–induced Nox4 expression. VSMCs or VSMCs expressing shRNA targeting LacZ (LacZ Si) and PKCζ (PKCζ Si) were cultured in DMEM containing HG (25 mmol/L) or normal glucose (NG; 5 mmol/L) plus 10% FBS and serum deprived for 16 h before changing to HG (25 mmol/L, NHG) or maintained in NG for 24 h. *A*: Before lysis, three different PKC inhibitors, PKCζ inhibitor (PKCzeta i; 10 μmol/L), PKCε inhibitor (PKCepsilon i; 20 μmol/L), and conventional PKC inhibitor (cPKC i; 1 μmol/L), were incubated for 2 h. Cell lysates were immunoblotted with an anti-Nox4 antibody. To control for loading, the blot was stripped and probed with an anti–β-actin antibody. *B*: Before cell lysis, a PKCζ inhibitor (10 μmol/L) was added for 2 h. Cell lysates were immunoblotted with anti-p419Src and anti-Src antibodies. *C*: Cell lysates obtained from cultures maintained in HG (25 mmol/L) were immunoblotted with anti-PKCζ (1:1,000) and β-actin antibodies. *D*: Cell lysates obtained from cultures maintained in NG or changed from NG to HG (NHG) were immunoblotted with anti-Nox4 and β-actin antibodies. *E*: Cell lysates prepared from cultures maintained in HG were immunoprecipitated with an anti-Src antibody, and protein oxidation level was measured according to the procedure described in RESEARCH DESIGN AND METHODS. *F*: Cell lysates prepared from cultures maintained in HG were immunoblotted with anti-p419Src and Src antibodies. IGF-I (100 ng/mL) was added as indicated. *G*: Different amounts of NF-κB inhibitor, as indicated, were preincubated for 1 h before changing glucose. Cell lysates were immunoblotted with anti-Nox4 and β-actin antibodies. The figures are representative of three independent experiments.

(Fig. 5*F*). IGF-I stimulation of MAP kinase and AKT activation was also impaired (Supplementary Fig. 4*B*). Importantly, the nuclear factor κB (NF-κB) inhibitor (BAY 11–7082) was able to prevent high glucose–induced Nox4 expression (Fig. 5*G*), suggesting that NF-κB is a transcription factor that mediates PKCζ induction of Nox4 expression during hyperglycemia.

Src oxidation and activation are required for mediating IGF-I downstream signaling and biological actions. In VSMCs, Src phosphorylates p52shc, which leads to MAP kinase activation (31). When VSMCs were exposed to NAC, IGF-I–stimulated p52shc tyrosine phosphorylation was attenuated (Fig. 6*A*). Because the IGF-I receptor phosphorylates Src homology 2 domain-containing protein tyrosine phosphatase substrate-1 (SHPS-1), a transmembrane scaffolding protein, and this is required for IGF-I–stimulated downstream signaling during hyperglycemia, we examined the effect of NAC on SHPS-1 phosphorylation. IGF-I–stimulated SHPS-1 tyrosine phosphorylation in the cells exposed to high glucose was not affected by NAC (Supplementary Fig. 4*C*), thus excluding the possibility that NAC functions as a general tyrosine kinase inhibitor. NAC preincubation also inhibited IGF-I–stimulated MAP kinase and AKT activation (Fig. 6*B* and *C*), and this led to attenuated IGF-I–stimulated cell proliferation (Fig. 6*D*). To confirm that the Nox4-mediated increase in ROS was required, cells expressing Nox4 shRNA were analyzed. IGF-I–stimulated MAP kinase and AKT activation were

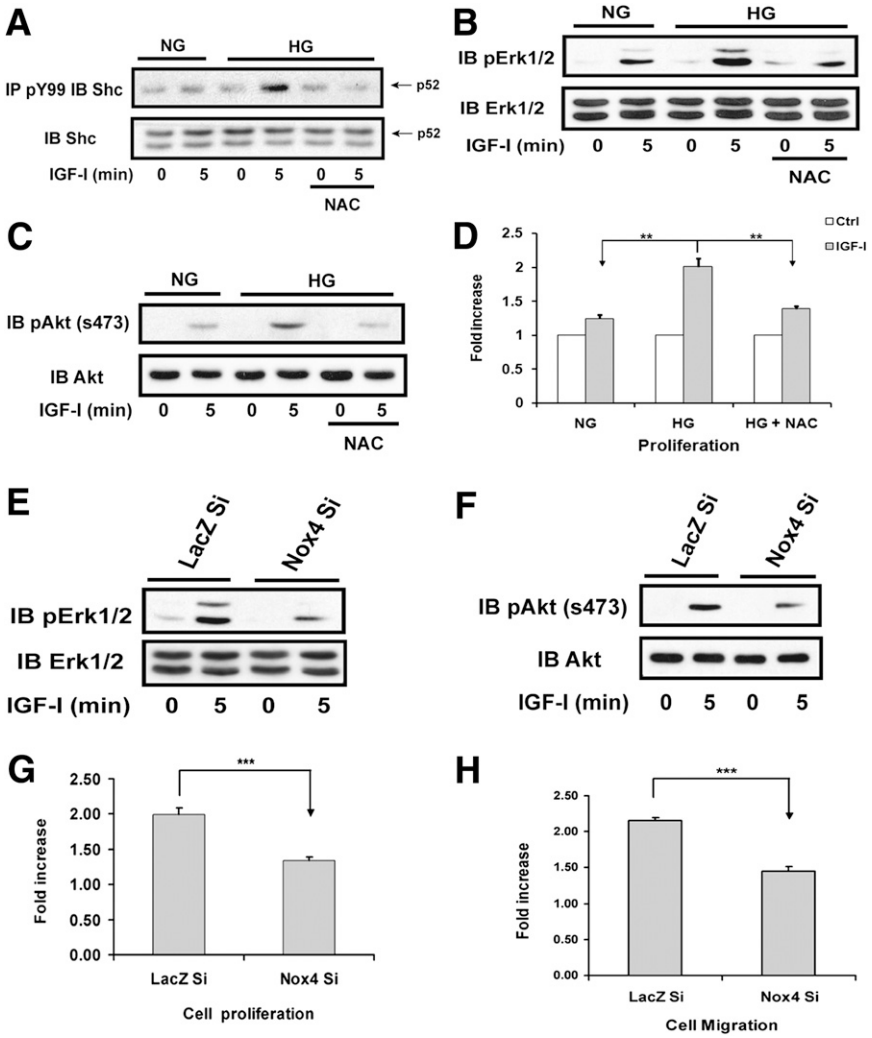

FIG. 6. Prevention of ROS generation impairs IGF-I signal transduction and biological actions. VSMCs were cultured in DMEM containing normal glucose (NG; 5 mmol/L) or high glucose (HG; 25 mmol/L) plus 10% FBS and serum deprived for 16 h before IGF-I treatment for the indicated times. For NAC treatment, 2 mmol/L NAC was added in serum-free DMEM and incubated for 16 h. *A*: Cell lysates were immunoprecipitated with an anti-PY99 antibody followed by immunoblotting with an anti-Shc (1:1,000) antibody. To control loading, the same amount of lysate protein was separated and immunoblotted using an anti-Shc antibody. *B* and *C*: Cell lysates were immunoblotted with anti-pErk1/2 (1:1,000) or pAKT(Ser473) (1:1,000) antibodies, respectively. To control for loading, the blots were stripped and probed with anti-Erk1/2 (1:1,000) or AKT (1:1,000) antibodies, respectively. *D*: VSMC proliferation was determined according to a procedure described in RESEARCH DESIGN AND METHODS. *E* and *F*: VSMCs expressing shRNA targeting LacZ (LacZ Si) or Nox4 (Nox4 Si) were cultured in DMEM containing HG plus 10% FBS and serum deprived for 16 h before IGF-I treatment for the indicated times. Cell lysates were immunoblotted with anti-pErk1/2 or pAKT(Ser473) antibodies, respectively. To control for loading, the blots were stripped and probed with anti-Erk1/2 or AKT antibodies, respectively. *G* and *H*: Cell proliferation and migration were determined as described in RESEARCH DESIGN AND METHODS. $^{**}P < 0.01$ and $^{***}P < 0.001$ indicate significant differences between two cell types or treatments. The figures are representative of three independent experiments.

impaired (Fig. 6*E* and *F*), and this resulted in attenuated cell proliferation (e.g., 34 ± 5% increase vs. 99 ± 9% increase; $P < 0.001$) (Fig. 6*G*) and migration (e.g., 45 ± 7% increase vs. 116 ± 4% increase; $P < 0.001$) (Fig. 6*H*) in response to IGF-I.

Hyperglycemia enhances IGF-I–stimulated Src oxidation and activation, which is prevented by PKCζ inhibition in diabetic mice. To verify that IGF-I stimulated Src oxidation and activation during hyperglycemia in vivo, diabetic mice were used. Serum glucose was increased (e.g., 331 ± 20 mg/dL; $n = 24$) in diabetic mice compared with normal mice (144 ± 9 mg/dL; $n = 12$). Nox4 and p22phox were increased in diabetic mice (Fig. 7*A*), whereas Nox1 expression was unchanged (Supplementary Fig. 4*D*). The PKCζ inhibitor decreased Nox4 in diabetic mice (Fig. 7*A*). Basal Src oxidation was increased 42 ± 12% in diabetic mice compared with normal mice ($P < 0.05$). IGF-I induced a further 138 ± 18% increase in diabetic mice ($P < 0.01$) whereas it had no effect in normal mice (Fig. 7*B*). The absolute Src oxidation level induced by IGF-I was 167 ± 34% greater in diabetic mice than normal mice ($P < 0.01$). The PKCζ inhibitor prevented the IGF-I–induced increase in Src oxidation in diabetic mice (e.g., 35 ± 21%, P = NS, vs. 138 ± 18%, $P < 0.01$) but had no effect on basal Src oxidation (Fig. 7*B*). Basal Src activation was increased 50 ± 14% in diabetic mice compared with normal mice ($P < 0.05$) but the absolute level of Src activation induced by IGF-I was increased 100 ± 29% ($P < 0.01$) (Fig. 7*C*). The PKCζ inhibitor inhibited this increase in response to IGF-I. A similar result was obtained when MAP kinase activation was determined (Fig. 7*D*). IGF-I significantly stimulated Nox4/p22phox complex formation in aorta from diabetic mice compared with the response of normal mice (e.g., 81 ± 9% increase vs. 23 ± 14% increase; $P < 0.01$), and the

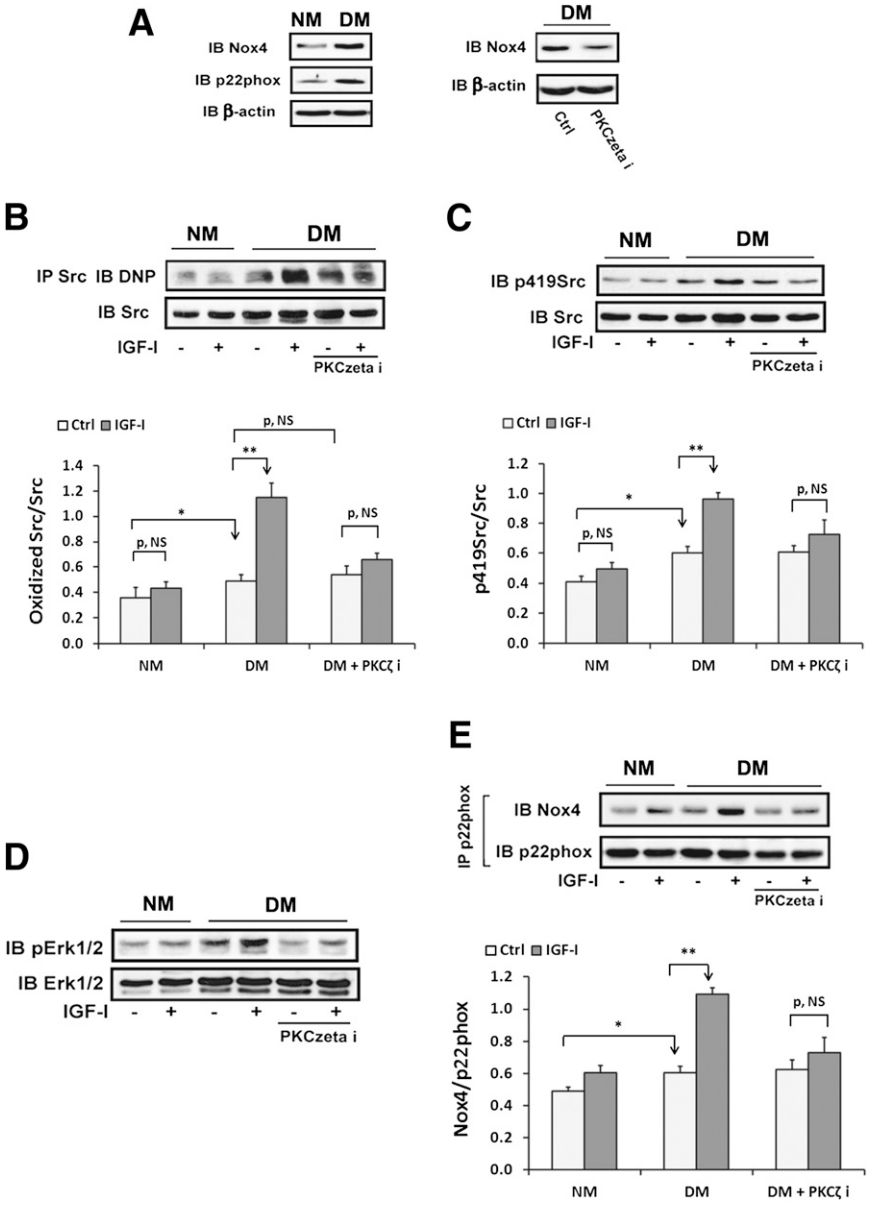

FIG. 7. Hyperglycemia enhances IGF-I–stimulated oxidation and activation of Src, which is prevented by a PKCζ inhibitor in vivo. The 8–10-week-old male C57/B6 mice were injected with streptozotocin (50 mg/kg i.p., diluted in citrate buffer; diabetic mice [DM]; $n = 24$) or with citrate buffer (normal mice [NM]; $n = 12$) for 5 consecutive days. The DM and NM were maintained for 2 weeks before analysis. Before they were killed, half of DM ($n = 12$) were injected daily with a PKCζ inhibitor (PKCzeta i; 2 mg/kg) for 2 days. In addition, half of normal ($n = 6$) or diabetic ($n = 12$) mice were injected with IGF-I (1 mg/kg body weight i.p., diluted in PBS) or PBS alone (control) for 15 min before they were killed by injection of Nembutal (100 mg/kg i.p.). Aortic extracts were prepared using the procedure described in RESEARCH DESIGN AND METHODS. *A*: Aortic extracts were immunoblotted using anti-Nox4, p22phox, and β-actin antibodies. *B*: The Src protein oxidation level was measured according to a procedure described in RESEARCH DESIGN AND METHODS. *C*: Aortic extracts were immunoblotted using an anti-p419Src antibody. The blot was stripped and probed with anti-Src antibody as a loading control. *D*: Aortic extracts were immunoblotted using an anti-pErk1/2 antibody. The blot was stripped and probed with anti-Erk1/2 antibody as a loading control. *E*: Aortic extracts were immunoprecipitated using an anti-p22phox antibody and immunoblotted using an anti-Nox4 antibody. The blot was stripped and probed with an anti-p22phox antibody as a loading control. The value of each bar is either the ratio of the scan value of oxidized Src divided by the value of Src (*B*), the ratio of the scan value of p419Src divided by the value of Src (*C*), or the ratio of the scan value of Nox4 divided by the value of p22phox (*E*). *$P < 0.05$ and **$P < 0.01$ indicate significant differences between two treatments or the two types of mice. The figures are representative of four independent experiments.

absolute level induced by IGF-I was 77 ± 20% greater than in normal mice ($P < 0.05$) (Fig. 7*E*). The PKCζ inhibitor prevented the effect of IGF-I in diabetic mice (e.g., 17 ± 4 vs. 81 ± 9% increase; $P < 0.01$). The diabetic mice had a 19 ± 6% increase in complex formation compared with nondiabetic mice ($P < 0.05$). To examine an IGF-I–stimulated biological action, Ki67 labeling (an indicator of cell proliferation) was analyzed. Hyperglycemia alone increased Ki67 labeling compared with normal mice (e.g., 57 ± 18% increase; $P < 0.05$). IGF-I stimulated a major increase in diabetic mice (e.g., 189 ± 32% increase; $P < 0.01$) but it had no significant effect in the normal mice. The PKCζ inhibitor prevented the IGF-I–stimulated increase in diabetic mice, suggesting that PKCζ activity is required for increased VSMC replication in vivo (Fig. 8).

DISCUSSION

In VSMCs exposed to hyperglycemia, IGF-I stimulates Src activation, and this is required for MAP kinase and AKT

activation (6,24). In the current study, we demonstrate that Src kinase activation requires the induction of a specific NAPDH oxidase, Nox4. Exposure of VSMCs to high glucose significantly increased expression of both Nox4 and p22phox, and PKCζ mediated the increase of Nox4. After exposure to hyperglycemia, the role of IGF-I appears to be to stimulate Nox4/p22phox complex formation, which is required for optimal ROS generation and Src activation. Reduction in Nox4 expression decreased Src oxidation, and this resulted in the loss of IGF-I–stimulated Src activation as well as attenuated cell proliferation and migration.

Previous studies have shown that Src kinase can be activated by multiple stimuli, such as angiotensin-II (14) and IGF-I (6). This study focused on the mechanism by which IGF-I stimulated Src activation during hyperglycemia and the role of Nox4-derived ROS. Crystal structure data show that disruption of intramolecular interactions in Src allows Y419 to be more accessible and thus fully activated (10). However, it is not clear what allows these domains to be become more accessible when Src is in the folded (inactive) conformation. That redox regulation may be involved is supported by studies that show that Src is activated by oxidation of cysteines and that this effect is reversible (32). One study implicated Nox4-derived ROS in angiotensin II–stimulated Src oxidation and activation (14). The proposed mechanism was that after oxidation, an intramolecular bond formed between two cysteines, which favored maintaining Src in the open conformation (15). In support of this hypothesis, a recent study revealed that oxidation of two neighboring cysteines leads to a conformational change in the SH3 domain, which alters the helix-sheet packing (33). Our results show that the increase in ROS induced by hyperglycemia leads to increased Src oxidation and that IGF-I stimulated a further increase in VSMCs and in diabetic mice. That Src oxidation is prerequisite for Src activation is supported by the observations that NAC prevented and H_2O_2 stimulated Src oxidation and Src kinase activation in response to IGF-I. Even though high glucose alone was sufficient to induce a major increase in Src oxidation, activation of Src in VSMCs also required stimulation by IGF-I. Because previous studies had shown that high glucose alone could activate Src (34,35), we examined the time course of Src activation. The results showed that high glucose–induced Src kinase activation lasted a short period of time (e.g., 10 min to 1 h) and that it subsequently returned to a basal level (Supplementary Fig. 4*H*). The increase Src oxidation induced by high glucose alone significantly exceeded Src activation after 14 h and at later time points. Furthermore, at time points later than 1 hour, IGF-I was required to induce a significant increase in Src activation. Our in vivo results also showed that optimal Src activation could only be obtained in IGF-I–treated diabetic mice. Because IGF-I induced a significantly greater increase in Src oxidation compared with glucose alone, it is possible that a high level of Src oxidation is required for its sustained activation. Alternatively, because the increased Nox4/p22phox association was important, it is possible that they colocalize with Src at a distinct location and that this localized increase in Src oxidation is required. We previously reported that Src (6) and Nox4 (36) are recruited to phosphorylated scaffold protein, SHPS-1, and that IGF-I receptor phosphorylation of SHPS-1 mediates this recruitment. Therefore this mechanism could account for the requirement for IGF-I to stimulate optimal Src activation. It is also possible that Src interacts with other binding partners, which allow oxidation of cysteines, such as Cys487, thus permitting Src activation (13).

Among the Nox isoforms, Nox4 and Nox1 are two major isoforms in vascular cells (19) and are a major source of intracellular ROS (18). However, the expression of Nox4 is abundant whereas Nox1 expression is relatively low in vascular cells (37). Consistently, we detected only a slight increase of Nox1 in VSMCs exposed to high glucose in vitro and no change in diabetic mice. More importantly, knockdown Nox1 in VSMCs exposed to high glucose did not affect IGF-I–stimulated Src oxidation and activation (Supplementary Fig. 4*E*–*G*). Therefore, we focused on Nox4-derived ROS. To generate ROS, Nox4 associates with p22phox (38). High glucose has been shown to increase both Nox4 and p22phox expression in endothelial cells (37,39), and our study clearly shows that high glucose significantly increased both Nox4 and p22phox expression in VSMCs. Because the change of Nox4 requires increased transcription, the induction in Nox4 by high glucose was delayed but it persisted for at least 24 h, and this is a key requirement for IGF-I to be able to stimulate a major increase in Nox4/p22phox complex formation.

IGF-I stimulated Nox4/p22phox complex formation in VSMCs exposed to high glucose and in diabetic mice. Because Nox4/p22phox complex formation is required for Nox4-derived ROS (38), this change appears to account for a significant part of the change in Src activation that occurred in response to IGF-I. By contrast, a recent study, that did not analyze the effect of glucose, showed that increased Nox4 expression accounted for IGF-I–induced ROS generation in rat VSMCs (20). However, in that study, increased ROS was detected after 5 min of IGF-I treatment whereas the increase of Nox4 expression required a 4-h exposure to IGF-I. Our results show that a short time exposure to IGF-I had a minimal effect on Src oxidation, Nox4 induction, p22phox/Nox4 association, or Src Y419 phosphorylation in cells maintained in 5 mmol/L glucose, and significant increases required exposure to high glucose. Therefore, the increase in Nox4 expression induced by high glucose appears to be required for IGF-I to stimulate a major increase in Nox4/p22phox complex formation. The requirement for Nox4-derived ROS for IGF-I–stimulated Src oxidation and activation was reinforced by our results obtained after Nox4 silencing. They showed that suppression of Nox4 significantly attenuated high glucose–induced ROS generation as well as IGF-I–stimulated Src oxidation and activation.

Previous studies have shown that different isoforms of PKC mediate high glucose–induced Nox4 expression in vivo (40) and in vitro (21,41). Utilizing specific PKC isoform inhibitors and silencing, our data show that PKCζ is responsible for the high glucose–induced Nox4 upregulation, Src oxidation, and activation in both VSMCs and diabetic mice. IGF-I–stimulated Nox4/p22phox complex formation was prevented when a PKCζ inhibitor was administrated in the diabetic mice. Because PKCζ has been shown to mediate NF-κB pathway activation (42,43), and NF-κB has been shown to mediate tumor necrosis factor-α (30) and hypoxia-induced (44) Nox4 expression in SMC, we postulated that PKCζ mediates high glucose–induced Nox4 expression via activation of the NF-κB pathway. In support of this hypothesis, our data show that an NF-κB inhibitor prevented high glucose–induced Nox4 expression.

The interaction between ROS and growth factor signal transduction has been previously reported. H_2O_2 generation is essential for mediating platelet-derived growth factor

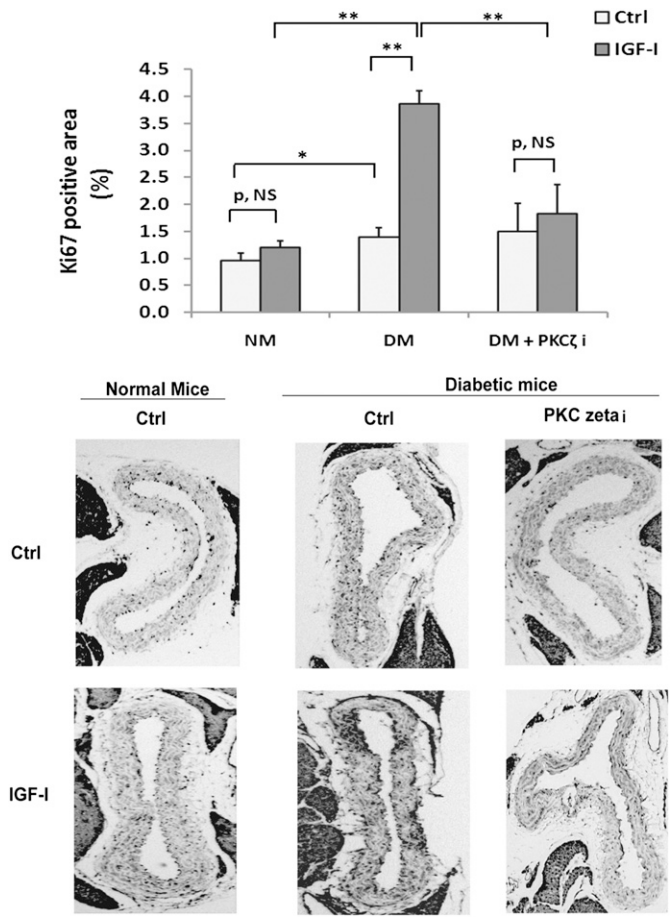

FIG. 8. Hyperglycemia enhances IGF-I–stimulated cell proliferation, which is prevented by a PKCζ inhibitor in vivo. The aortas were obtained from the mice described in the Fig. 7 legend and fixed in 4% paraformaldehyde overnight for paraffin-embedded section preparation. After staining with an anti-Ki67 antibody, the number of proliferating cells in the layer was measured using NIH imageJ software and expressed as the percentage of ring area that was Ki67 positive (Ki67 labeling area/total aortic ring area). The mean values ± SE from six mice per treatment group (with four sections measured per mouse) are shown graphically, and representative images are also shown. *$P < 0.05$ and **$P < 0.01$ indicate significant differences when the two treatments were compared.

signal transduction in VSMCs (45) and epidermal growth factor signaling in epithelial cells (46). The mechanism that was proposed initially was that H_2O_2 inhibited the activation of tyrosine phosphatases, including protein tyrosine phosphatase 1B and SHP-2, which altered the balance between kinase and phosphatase activity and resulted in enhanced actions. Recent studies have indicated that increased ROS leads to Src oxidation, and activated Src directly phosphorylates epidermal growth factor receptor on tyrosine 845 (47). Our results demonstrate that generation of ROS is required for mediating IGF-I–stimulated Src activation as well as downstream signaling and biological actions. Although our in vivo data indicated that hyperglycemia alone was able to induce an increase in cell proliferation in vivo, this is not surprising because these cells secrete growth factors, such as TGF-β, and they are exposed to plasma, which contains several mitogens, including IGF-I. However, a more robust proliferative response was detected after IGF-I treatment in diabetic mice, and the PKCζ inhibitor prevented this response. These results strongly support the conclusion that enhanced ROS generation and Src oxidation in response to hyperglycemia play vital roles in mediating the VSMC proliferative response to IGF-I. These findings are relevant to diabetic patients who are receiving insulin because insulin has been shown to increase serum IGF-I concentrations in diabetic patients (48) and diabetic animals (49).

In summary, our study provides direct evidence for IGF-I–stimulated Src oxidation during hyperglycemia, which is required for Src activation in response to IGF-I in VSMCs. Hyperglycemia induces Nox4 and p22phox expression, and IGF-I induces Nox4 and p22phox complex formation, leading to increased ROS generation and Src activation. High glucose induces Nox4 upregulation in a PKCζ/NF-κB–dependent manner. Disruption of ROS generation via either knockdown of Nox4 or PKCζ or preincubation with NAC impairs Src oxidation and activation in response to IGF-I, and this leads to impaired IGF-I signal transduction and biological actions. This study defines the molecular events that lead to hyperglycemia/IGF-I–stimulated ROS generation and Src activation in VSMCs and blood vessels of diabetic mice, and provides a framework for developing methods to modify the vascular response to hyperglycemic stress.

ACKNOWLEDGMENTS

This work was supported by a grant from the National Institutes of Health (AG-02331).

No potential conflicts of interest relevant to this article were reported.

G.X. performed the experiments and wrote the manuscript. X.S., L.A.M., C.W., and K.G. performed the experiments. D.R.C. wrote and edited the manuscript, contributed to research design and discussion of the results, and is the guarantor of this article.

The authors thank Laura Lindsey (University of North Carolina at Chapel Hill) for her help in preparing the article.

REFERENCES

1. Brownlee M. Biochemistry and molecular cell biology of diabetic complications. Nature 2001;414:813–820
2. Nishikawa T, Edelstein D, Du XL, et al. Normalizing mitochondrial superoxide production blocks three pathways of hyperglycaemic damage. Nature 2000;404:787–790
3. Maile LA, Capps BE, Ling Y, Xi G, Clemmons DR. Hyperglycemia alters the responsiveness of smooth muscle cells to insulin-like growth factor-I. Endocrinology 2007;148:2435–2443
4. Ross R. Atherosclerosis—an inflammatory disease. N Engl J Med 1999;340:115–126
5. Radhakrishnan Y, Maile LA, Ling Y, Graves LM, Clemmons DR. Insulin-like growth factor-I stimulates Shc-dependent phosphatidylinositol 3-kinase activation via Grb2-associated p85 in vascular smooth muscle cells. J Biol Chem 2008;283:16320–16331
6. Lieskovska J, Ling Y, Badley-Clarke J, Clemmons DR. The role of Src kinase in insulin-like growth factor-dependent mitogenic signaling in vascular smooth muscle cells. J Biol Chem 2006;281:25041–25053
7. Boney CM, Sekimoto H, Gruppuso PA, Frackelton AR Jr. Src family tyrosine kinases participate in insulin-like growth factor I mitogenic signaling in 3T3-L1 cells. Cell Growth Differ 2001;12:379–386
8. Li SL, Reddy MA, Cai Q, et al. Enhanced proatherogenic responses in macrophages and vascular smooth muscle cells derived from diabetic db/db mice. Diabetes 2006;55:2611–2619
9. Murphy SM, Bergman M, Morgan DO. Suppression of c-Src activity by C-terminal Src kinase involves the c-Src SH2 and SH3 domains: analysis with *Saccharomyces cerevisiae*. Mol Cell Biol 1993;13:5290–5300
10. Xu W, Doshi A, Lei M, Eck MJ, Harrison SC. Crystal structures of c-Src reveal features of its autoinhibitory mechanism. Mol Cell 1999;3:629–638
11. Alonso G, Koegl M, Mazurenko N, Courtneidge SA. Sequence requirements for binding of Src family tyrosine kinases to activated growth factor receptors. J Biol Chem 1995;270:9840–9848

12. Alper O, Bowden ET. Novel insights into c-Src. Curr Pharm Des 2005;11:1119–1130
13. Giannoni E, Taddei ML, Chiarugi P. Src redox regulation: again in the front line. Free Radic Biol Med 2010;49:516–527
14. Block K, Eid A, Griendling KK, Lee DY, Wittrant Y, Gorin Y. Nox4 NAD(P)H oxidase mediates Src-dependent tyrosine phosphorylation of PDK-1 in response to angiotensin II: role in mesangial cell hypertrophy and fibronectin expression. J Biol Chem 2008;283:24061–24076
15. Giannoni E, Buricchi F, Raugei G, Ramponi G, Chiarugi P. Intracellular reactive oxygen species activate Src tyrosine kinase during cell adhesion and anchorage-dependent cell growth. Mol Cell Biol 2005;25:6391–6403
16. Rosado JA, Redondo PC, Salido GM, Gómez-Arteta E, Sage SO, Pariente JA. Hydrogen peroxide generation induces pp60src activation in human platelets: evidence for the involvement of this pathway in store-mediated calcium entry. J Biol Chem 2004;279:1665–1675
17. Brown DI, Griendling KK. Nox proteins in signal transduction. Free Radic Biol Med 2009;47:1239–1253
18. Ellmark SH, Dusting GJ, Fui MN, Guzzo-Pernell N, Drummond GR. The contribution of Nox4 to NADPH oxidase activity in mouse vascular smooth muscle. Cardiovasc Res 2005;65:495–504
19. Basuroy S, Bhattacharya S, Leffler CW, Parfenova H. Nox4 NADPH oxidase mediates oxidative stress and apoptosis caused by TNF-alpha in cerebral vascular endothelial cells. Am J Physiol Cell Physiol 2009;296:C422–C432
20. Meng D, Lv DD, Fang J. Insulin-like growth factor-I induces reactive oxygen species production and cell migration through Nox4 and Rac1 in vascular smooth muscle cells. Cardiovasc Res 2008;80:299–308
21. Xia L, Wang H, Goldberg HJ, Munk S, Fantus IG, Whiteside CI. Mesangial cell NADPH oxidase upregulation in high glucose is protein kinase C dependent and required for collagen IV expression. Am J Physiol Renal Physiol 2006;290:F345–F356
22. Yano M, Hasegawa G, Ishii M, et al. Short-term exposure of high glucose concentration induces generation of reactive oxygen species in endothelial cells: implication for the oxidative stress associated with postprandial hyperglycemia. Redox Rep 2004;9:111–116
23. Xi G, Shen X, Clemmons DR. p66shc negatively regulates insulin-like growth factor I signal transduction via inhibition of p52shc binding to Src homology 2 domain-containing protein tyrosine phosphatase substrate-1 leading to impaired growth factor receptor-bound protein-2 membrane recruitment. Mol Endocrinol 2008;22:2162–2175
24. Xi G, Shen X, Radhakrishnan Y, Maile L, Clemmons D. Hyperglycemia-induced p66shc inhibits insulin-like growth factor I-dependent cell survival via impairment of Src kinase-mediated phosphoinositide-3 kinase/AKT activation in vascular smooth muscle cells. Endocrinology 2010;151:3611–3623
25. Maile LA, Capps BE, Miller EC, Aday AW, Clemmons DR. Integrin-associated protein association with SRC homology 2 domain containing tyrosine phosphatase substrate 1 regulates igf-I signaling in vivo. Diabetes 2008;57:2637–2643
26. Petit I, Goichberg P, Spiegel A, et al. Atypical PKC-zeta regulates SDF-1-mediated migration and development of human CD34+ progenitor cells. J Clin Invest 2005;115:168–176
27. Nam TJ, Busby WH Jr, Rees C, Clemmons DR. Thrombospondin and osteopontin bind to insulin-like growth factor (IGF)-binding protein-5 leading to an alteration in IGF-I-stimulated cell growth. Endocrinology 2000;141:1100–1106
28. Jones JI, Prevette T, Gockerman A, Clemmons DR. Ligand occupancy of the alpha-V-beta3 integrin is necessary for smooth muscle cells to migrate in response to insulin-like growth factor. Proc Natl Acad Sci USA 1996;93:2482–2487
29. Schröder K. Isoform specific functions of Nox protein-derived reactive oxygen species in the vasculature. Curr Opin Pharmacol 2010;10:122–126
30. Manea A, Tanase LI, Raicu M, Simionescu M. Transcriptional regulation of NADPH oxidase isoforms, Nox1 and Nox4, by nuclear factor-kappaB in human aortic smooth muscle cells. Biochem Biophys Res Commun 2010;396:901–907
31. Ling Y, Maile LA, Lieskovska J, Badley-Clarke J, Clemmons DR. Role of SHPS-1 in the regulation of insulin-like growth factor I-stimulated Shc and mitogen-activated protein kinase activation in vascular smooth muscle cells. Mol Biol Cell 2005;16:3353–3364
32. Rhee SG, Bae YS, Lee SR, Kwon J. Hydrogen peroxide: a key messenger that modulates protein phosphorylation through cysteine oxidation. Sci STKE 2000;2000:pe1
33. Zimmermann J, Kühne R, Sylvester M, Freund C. Redox-regulated conformational changes in an SH3 domain. Biochemistry 2007;46:6971–6977
34. Schaeffer G, Levak-Frank S, Spitaler MM, et al. Intercellular signalling within vascular cells under high D-glucose involves free radical-triggered tyrosine kinase activation. Diabetologia 2003;46:773–783
35. Huang Q, Sheibani N. High glucose promotes retinal endothelial cell migration through activation of Src, PI3K/Akt1/eNOS, and ERKs. Am J Physiol Cell Physiol 2008;295:C1647–C1657
36. Shen X, Xi G, Radhakrishnan Y, Clemmons DR. Identification of novel SHPS-1-associated proteins and their roles in regulation of insulin-like growth factor-dependent responses in vascular smooth muscle cells. Mol Cell Proteomics 2009;8:1539–1551
37. Sorescu D, Weiss D, Lassègue B, et al. Superoxide production and expression of nox family proteins in human atherosclerosis. Circulation 2002;105:1429–1435
38. Martyn KD, Frederick LM, von Loehneysen K, Dinauer MC, Knaus UG. Functional analysis of Nox4 reveals unique characteristics compared to other NADPH oxidases. Cell Signal 2006;18:69–82
39. Chai D, Wang B, Shen L, Pu J, Zhang XK, He B. RXR agonists inhibit high-glucose-induced oxidative stress by repressing PKC activity in human endothelial cells. Free Radic Biol Med 2008;44:1334–1347
40. Yang J, Lane PH, Pollock JS, Carmines PK. Protein kinase C-dependent NAD(P)H oxidase activation induced by type 1 diabetes in renal medullary thick ascending limb. Hypertension 2010;55:468–473
41. Kwan J, Wang H, Munk S, Xia L, Goldberg HJ, Whiteside CI. In high glucose protein kinase C-zeta activation is required for mesangial cell generation of reactive oxygen species. Kidney Int 2005;68:2526–2541
42. Win HY, Acevedo-Duncan M. Atypical protein kinase C phosphorylates IKKalphabeta in transformed non-malignant and malignant prostate cell survival. Cancer Lett 2008;270:302–311
43. LaVallie ER, Chockalingam PS, Collins-Racie LA, et al. Protein kinase Czeta is up-regulated in osteoarthritic cartilage and is required for activation of NF-kappaB by tumor necrosis factor and interleukin-1 in articular chondrocytes. J Biol Chem 2006;281:24124–24137
44. Lu X, Murphy TC, Nanes MS, Hart CM. PPARgamma regulates hypoxia-induced Nox4 expression in human pulmonary artery smooth muscle cells through NF-kappaB. Am J Physiol Lung Cell Mol Physiol 2010;299:L559–L566
45. Sundaresan M, Yu ZX, Ferrans VJ, Irani K, Finkel T. Requirement for generation of H2O2 for platelet-derived growth factor signal transduction. Science 1995;270:296–299
46. Huo Y, Qiu WY, Pan Q, Yao YF, Xing K, Lou MF. Reactive oxygen species (ROS) are essential mediators in epidermal growth factor (EGF)-stimulated corneal epithelial cell proliferation, adhesion, migration, and wound healing. Exp Eye Res 2009;89:876–886
47. Biscardi JS, Maa MC, Tice DA, Cox ME, Leu TH, Parsons SJ. c-Src-mediated phosphorylation of the epidermal growth factor receptor on Tyr845 and Tyr1101 is associated with modulation of receptor function. J Biol Chem 1999;274:8335–8343
48. Grandis M, Nobbio L, Abbruzzese M, et al. Insulin treatment enhances expression of IGF-I in sural nerves of diabetic patients. Muscle Nerve 2001;24:622–629
49. Guney E, Kisakol G, Oge A, Yilmaz C, Kabalak T. Effects of insulin and sulphonylureas on insulin-like growth factor-I levels in streptozotocin-induced diabetic rats. Neuroendocrinol Lett 2002;23:437–439
50. Gockerman A, Clemmons DR. Porcine aortic smooth muscle cells secrete a serine protease for insulin-like growth factor binding protein-2. Circ Res 1995;76:514–521